Determination of Surface Structure by LEED

Edited by

P. M. Marcus

Thomas J. Watson IBM Research Center
Yorktown Heights, New York

and

F. Jona

SUNY at Stony Brook
Stony Brook, New York

PLENUM PRESS • NEW YORK AND LONDON

Library of Congress Cataloging in Publication Data

Conference on Determination of Surface Structure by LEED (1980: Thomas J. Watson IBM Research Center)
Determination of surface structure by LEED.

(The IBM research symposia series)
Includes bibliographical references and index.
1. Surfaces (Physics)—Technique—Congresses. 2. Low-energy electron diffraction—Congresses. 3. Surface chemistry—Technique—Congresses. I. Marcus, P. M.,1921-. II. Jona, F. III. Title. IV. Series.
QC173.4.S94C66 1980 530.4 84-3481
ISBN 0-306-41664-6

Proceedings of a conference on Determination of Surface Structure by LEED, held June 19–20, 1980, at the Thomas J. Watson IBM Research Center, Yorktown Heights, New York

CONTENTS

1. Intensity Theory: Formulations and Calculations

3. Instrumentation and Data Acquisition

4. Defects, Potentials, Bonding

INFLUENCE OF STATISTICALLY DISTRIBUTED POINT DEFECTS ON LEED INTENSITIES

Wolfgang Moritz

Institut f. Kristallographie u. Mineralogie
Universität München, West Germany

In honour of Prof. Dr. H. Jagodzinski's 65th birthday

INTRODUCTION

Real surfaces as well as three-dimensional crystals always have a certain number of defects which are usually neglected in LEED studies. The reason is that defects often are not easily visible in the diffraction picture. First, there is the low resolution power of normal LEED instruments which limits the correlation lengths directly visible on the fluorescent screen, and second, it is experimentally difficult to distinguish between an elastic and inelastic background. Because of the latter the density of defects distributed at random, which cause an increase in the elastic background, can only be qualitatively estimated from background measurements. Furthermore, the measured I-V curves of the sharp spots agree quite often rather well with calculated ones, even in cases where it is known that the surface contains impurities or is far from being perfectly flat, while the calculation is always done on the assumption of a perfect crystal.

Therefore it is often concluded that LEED is not very sensitive to surface defects, a conclusion which has already been proven erroneous since the first difficulty - the limited transfer width - can be overcome by an improvement of experimental techniques and careful analysis of the angular profiles of the incident and the diffracted beams [1-3]. In this case the resolution can be considerably increased and LEED may well be used in studying the distribution of various kinds of surface defects as long as they produce a change in the beam profiles. It has been shown previously that multiple scatter-

ing effects do not produce special features in the angular distribution of diffracted beams [4]. Therefore the analysis of beam profiles may be done in a kinematic or quasi-kinematic way.

In case of a random distribution of point defects, such as vacancies or adsorbed atoms, the situation is much more difficult. There are still sharp spots visible in the diffraction picture and an increase in background occurs. The quantitative analysis of the background intensity is somewhat uncertain and calculation of spot intensities involves a multiple scattering theory.

In kinematic theory only small changes in the beam intensities caused by point defects are predicted, and this influence is independent of energy as well as diffraction conditions. The diffraction intensity from a random distribution of scatterers still placed at lattice sites is given by [5]

$$I(\underline{K},\underline{K}') \sim |\langle f\rangle|^2 \delta(\underline{K}-\underline{K}'-\underline{g}) + \{\langle|f|^2\rangle - |\langle f\rangle|^2\}$$

The first term represents a sharp spot proportional to the square of an average amplitude and is due to the fact that a fixed spacing exists for the mean position of each atom. The second term is a uniform background proportional to the mean square deviation of scattering amplitudes. The average amplitude is given by

$$\langle f\rangle = \sum_n p_n f_n$$

where p_n are the a priori probabilities for the occurrence of the different scatterers.

If only a small amount of impurities is present, the average amplitude is only slightly changed compared to the clean surface. In case of vacancies the intensity of all beams is just a bit lowered. The I-V curves only get a different scaling but otherwise remain unchanged.

By multiple scattering the change in intensity of the sharp spots will become energy-dependent and may be larger or smaller than predicted by the kinematic theory. Of course, it remains true that only sharp spots are visible beneath a uniform background. There are no additional spots produced by multiple scattering and a diffuseness would be due to correlations of defects, not to multiple scattering. A multiple scattering calculation of the influence of point defects on LEED intensities is of interest for two reasons. First,

whether point defects can be detected and analyzed by LEED and under what conditions this can be done, and second, to get a ratio of errors made in the usual analysis by neglecting vacancies and impurities.

MULTIPLE SCATTERING THEORY

As a result of multiple scattering the effective scattering amplitude of a certain atom, which describes the total flux leaving the atom, is no longer related to the single potential only, but to its environment too. The problem has to be solved selfconsistently. In the case of perfect crystals this can be done exactly if there are not too many atoms in the unit cell. Several computational methods have been developed, the calculation can be done in k-space and in real space. The latter is used here, following the t-matrix formulation described by Beeby [6]. This method of calculation has the advantage that the t-matrices depend on the incoming wave only and not on the outgoing waves. The same formalism has been used in the description of scattering resulting from correlated defects [7,8].

The presence of defects destroys the translation symmetry of the surface, each atom in principal is surrounded by a different environment and accordingly the effective scattering amplitude is different for each atom. An exact solution is no longer available in practice, even though due to the strong damping of the electron wave inside the crystal the distance for multiple scattering processes is limited. It is therefore necessary to introduce averages to make the problem tractable. Averages of multiple scattering processes can be taken in different, more or less restrictive ways, which will be discussed below.

Once the effective scattering amplitudes are calculated, regardless of approximation, the diffracted intensity is given by the same formula as in the kinematic case.

Each scattering amplitude $f_n(\underline{k},\underline{k}')$ now individually depends on the incoming and outgoing waves $\underline{k}$ and $\underline{k}'$, and their number, of course, is increased when different environments can be distinguished.

Single site approximation

The most restrictive average is taken by a complete decoupling of a given site and its surrounding. Each atom is represented by an average potential embedded in an average uniform medium. This is a single site approximation since correlations in the multiple scattering process are completely

neglected. In band structure calculations of alloys it is known as the average t-matrix approximation (ATA) [9].

In case of vacancies or substitutional occupancy of lattice sites the average atom in a layer or subplane is represented by a single t-matrix

$$\begin{aligned} \langle \tau \rangle &= \langle t \rangle + \langle t \rangle G^{sp} \langle \tau \rangle \\ \langle t \rangle &= \sum_n p_n t_n \end{aligned} \qquad (1)$$

where $\langle t \rangle$ is the average single scattering matrix and p_n are the corresponding probabilities.

$$t_{LL'n} = e^{i\eta_{\ell,n}} \sin \eta_{\ell,n} \delta_{LL'} \qquad L \hat{=} (\ell m)$$

is a diagonal matrix describing a single scattering event, and G^{sp} is the interplanar propagator, η_ℓ are the phase shifts.

The average reflection and transmission matrices are then obtained in the usual way [10]

$$\langle M^{\pm}_{g'g} \rangle = \frac{8\pi^2 i}{|K| \Lambda K'_\perp} \sum_{LL'} (-1)^m Y_{\ell -m}(\Omega_K) \langle \tau \rangle_{LL'} Y_{\ell' m'}(\Omega_{K'}) \qquad (2)$$

The set of linear equations (1) could also be easily extended to several layers, using exactly the same formalism as for a perfect crystal. The average reflection and transmission matrices may be added to an otherwise perfect crystal, using a layer-doubling- or RFS-scheme.

The advantage of the average t-matrix approximation is, that it easily applies to any of the existing LEED programs; there is practically no additional effort. Furthermore, it can be applied to any density of defects and to alloys as well. The average t-matrix approximation should work well when multiple scattering effects are weak, however, it is known that in most cases this cannot be supposed and one expects the single site approximation to be not sufficient for most LEED applications.

Site-dependent approximation

A far better approximation than the single site approximation can be done by dividing the environment of a point defect into a near region and an outer region. Within a near region, nearest, or next nearest neighbours, all multiple

scattering processes are calculated exactly and only the outer region is treated by an average t-matrix. That means, not a single site but a whole cluster of atoms is surrounded by an average medium.

The basic consideration for this approximation is the fact that the most important contribution to the total scattering amplitude is due to single scattering, and multiple scattering within the immediate neighbourhood of an atom. The validity of this assumption is demonstrated in Fig. (1), here the lattice sum for interlayer scattering has been cut off at nearest and next nearest neighbours. To reach convergence, of course,

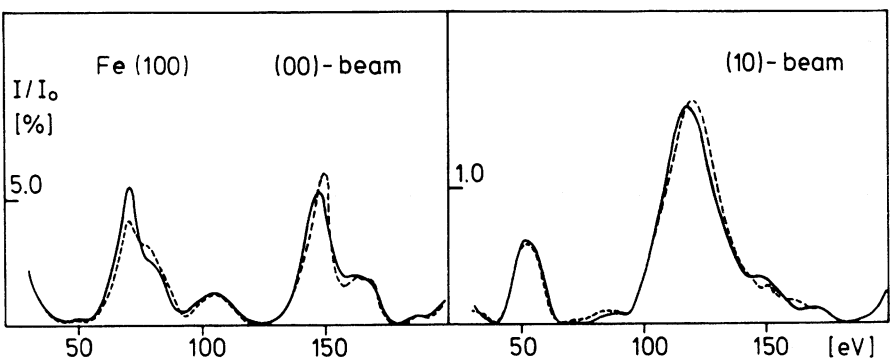

Fig. 1 Calculated I-V spectra for Fe(100) at normal incidence.
Solid line: full dynamical calculation
Broken line: only nearest and next nearest neighbours are taken for interplanar scattering.

usually several hundred atoms have to be included, but as can be seen, the curves with next nearest neighbours fit the exact calculation rather well, though the rest of the plane is completely neglected. The approximation should be even better, taking at least the single scattering amplitude for the rest of the plane.

A site-dependent approximation may be useful also for complicated ordered structures. It is not necessary to take only the environment within one plane, several layers, of course, complicate the calculation and it is completely unnecessary for simple structures since then the interlayer scattering can be done in reciprocal space, but for complicated structures a great number of beams occur and a t-matrix calculation with a restricted lattice sum will be easier.

In general, for all different sites, that means, for all possible different environments of an atom, an effective scattering amplitude has to be calculated separately. It has also the advantage that statistical correlations are easily introduced [7], the different configurations just have to be linked with the appropriate probabilities and, since the t-matrices do not depend on the diffracted wave, the beam profiles are obtained too without further effort. In practice, however, the problem becomes instantly unsolvable because of the number of different configurations. There are special cases where the size of the matrices to be inverted is reduced such that a calculation is possible indeed. We are facing such a case in one-dimensional disorder where the number of different sites is greatly reduced. Another case is given by dilute point defects where only one type of configuration remains. This problem will be discussed here. A further application may be possible for perfectly ordered crystals with large unit cells. Here the number of different neighbourhoods may be less than the number of atoms in the unit cell. For each configuration the scattering amplitude can be calculated independently and the computing time scale remains linear to the number of configurations. As mentioned above, such an approximate solution may be useful when applied to large unit cells where the number of beams is too large to be handled in ordinary type computers.

In general the t-matrices for N atoms embedded in an average medium are given by the following set of equations

$$\tau_n = t_n + \sum_m^{1,N} t_n G_{nm}(\underline{R}_n - \underline{R}_m)\, e^{-i\underline{k}(\underline{R}_n - \underline{R}_m)}\, \tau_m + \sum_R{}' G(\underline{R}_n - \underline{R})\, e^{-i\underline{k}(\underline{R}_n - \underline{R})} \langle \tau \rangle \qquad (3)$$

The prime on the summation symbol indicates that only those vectors R pointing to atoms of the average region are included. The average matrix $\langle \tau \rangle$ may be calculated independently, using the average t-matrix approximation if this facilitates the calculation.

A cluster containing N atoms still affords the inversion of an $(N \cdot n_l^2) \times (N \cdot n_l^2)$ matrix, where n_l is the number of phase shifts. Further reduction in size is necessary to make the calculation possible.

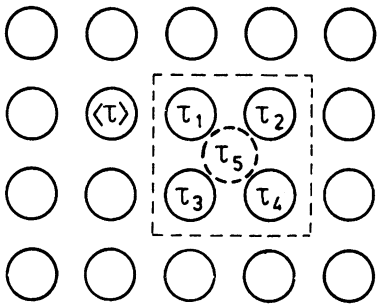

Fig. 2 Illustration of the site-dependent approximation. The nearest neighbours of an adsorbed atom all get different t-matrices, the atoms in the outer region all get the same averaged t-matrix.

How this can be done, using the symmetry of the crystal, may be discussed in some detail for an adatom and its nearest neighbours shown in Fig. (2). If the atom is adsorbed in the fourfold site only two different scattering matrices remain of a total of five, the others can be obtained by rotation matrices. The scattering amplitude $f(\underline{K},\underline{K}')$ must be the same for atoms 1 and 2 in Fig. (3) if $\underline{K}$ and $\underline{K}'$ are both rotated by $\pi/2$.
With

$$f_1(\underline{k},\underline{k}') = \frac{8\pi^2}{|k|} \sum_{LL'} (-1)^m Y_{\ell -m}(\vartheta_k, \varphi_k)\, \tau_{1,LL'}\, Y_{\ell' m'}(\vartheta_{k'}, \varphi_{k'})$$

and

$$Y_{\ell m}(\vartheta, \varphi) = \Theta_{\ell m}(\vartheta)\, e^{im\varphi}$$

it follows immediately that

$$\tau_2 = D\, \tau_1 D^{-1}$$

with

$$D_{LL'} = e^{im\frac{\pi}{2}}\, \delta_{LL'}$$

a similar relation follows directly from the definition of the propagator matrices

$$G(\underline{P}) = \sum_{L''} 4\pi k\, C(L,L';L'')\, i^{\ell} h_{\ell''}(|k|\cdot|P|)\, Y_{\ell''m''}(\Omega_P)$$

$$G(\underline{P}_{13}) = D\, G(\underline{P}_{12})\, D^{-1}$$

The set of eq. (3) can then be solved for two matrices only. Using a short notation, eq. (3) reduces to

$$\tau_1 = t_1 + t_1 G^{12} D \tau_1 D^{-1} + t_1 G^{13} D^2 \tau_1 D^{-2} + t_1 G^{14} D^3 \tau_1 D^{-3} + t_1 G^{15} \tau_5 + t_1 G_1' \langle\tau\rangle$$

$$\tau_5 = t_5 + t_5 G^{51} \tau_1 + t_5 G^{52} D \tau_1 D^{-1} + t_5 G^{53} D^2 \tau_1 D^{-2} + t_5 G^{54} D^3 \tau_1 D^{-3} + t_5 G_5' \langle\tau\rangle \quad (4)$$

It should be noted that multiple scattering between adatoms is neglected here, otherwise some additional terms would occur, causing no principal difficulty.

Further reduction in computing time and core size can be achieved by use of a symmetry relation for the propagator matrices

$$G_{LL'}(\underline{P}) = (-1)^{\ell+\ell'} G_{LL'}(-\underline{P})$$

Since only 4 different values in the rotation matrix D occur, eq. (4) can be solved easier than the general eq. (3), but still 4 Gaussian elimimations are necessary.

There is only one solution necessary for the whole set of incoming waves, since the phase-factors can be factorized in the same way described by Tong and Van Hove [11].

If we assume a density α of adatoms with α small enough that the probability for two neighbouring adatoms is negligible, then the average reflection and transmission matrix for the whole layer is

$$\langle \underline{\underline{M}}^{t}_{g'g} \rangle = \frac{8\pi^2 i}{|k|\cdot A\cdot k_\perp} \sum_{LL'} (-1)^m Y_{\ell-m}(\Omega_{k_g}) \Big\{ \langle\tau\rangle (1-4\alpha) + \alpha \sum_{n}^{1,4} \tau_n + \alpha\, e^{i(\underline{k}_g - \underline{k}_{g'})\underline{d}_5} \tau_5 \Big\}_{LL'} Y_{\ell'm'}(\Omega_{k_{g'}})$$

The case of vacancies can be treated completely equivalent. Here even next nearest neighbours can be included with the same computational effort as for the adatoms.

RESULTS

Model calculations for two types of point defects, vacancies, and adsorbed atoms, have been done for Fe(100), and for vacancies only in the case of Au(100). A defect density of 5 % and 10 % of a monolayer has been taken, though at 10 % correlated defects cannot be left off anymore, that means, the probability for the occurrence of clusters containing two or more vacancies or adatoms is much too high to be neglected. However, one can assume that a full calculation would not give a substantial change of the results.

All calculations were performed at normal incidence. Up to 8 phase shifts were used, obtained from band structure potentials [12]. Interlayer scattering was calculated by the layer-doubling method including a maximum of 24 symmetrically independent beams. The real part of the inner potential has

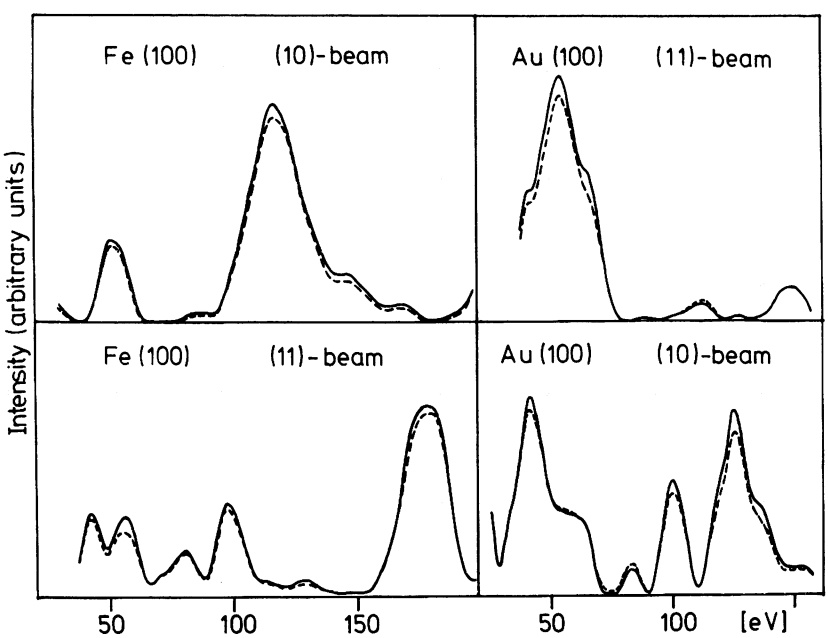

Fig. 3 Influence of vacancies on I-V spectra from Fe(100) and unreconstructed Au(100) at normal incidence.
Solid line: perfect crystal
Broken line: 5 % vacancies in the top layer

been set to zero and the imaginary part to 4 eV, independent of energy. Bulk Debye temperatures have been taken for all layers, 400 K for iron, 170 K for gold.

Fig. (3) shows the influence of 5 % vacancies in the top layer. The average t-matrix approximation gives nearly the same results as the calculation which includes nearest and next nearest neighbours. The broken line in Fig. (3) refers to both approximations. The kinematic calculation would have given a general energy-independent lowering of intensities, the multiple scattering calculation shows some changes in the I-V curves, as expected, but the influence is generally very small. Results for other beams are similar, also the strongly scattering material like gold does not produce larger effects.

As adatoms iron and nitrogen have been chosen and they were put in the fourfold hollow site on top of the first layer. For the iron atom the bulk distance has been assumed, and for the nitrogen atom, somewhat arbitrary, a layer spacing of 0.7 Å has been taken. No changes in positions of the atoms around the adatom or the vacancy have been considered.

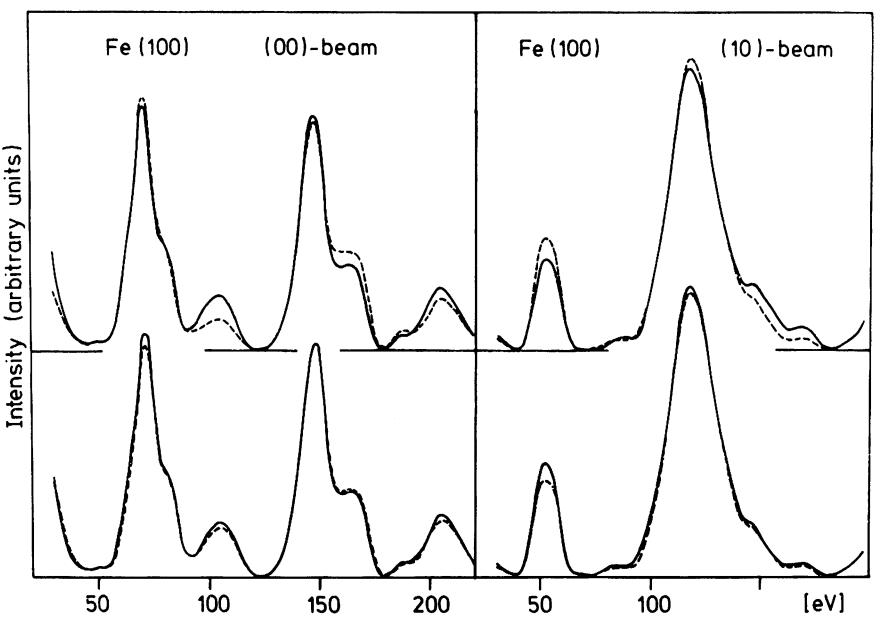

Fig. 4 Influence of adatoms on I-V spectra at normal incidence. (see text for explanation)

The onset of damping has been chosen differently for adatoms and vacancies. In the case of adatoms the damping starts in the plane of adatoms, and in the case of vacancies half a layer distance in front of the top layer. The comparison with the perfect crystal is always made by choosing the same damping conditions.

In the upper left and upper right panel of Fig. (4) the influence of 10 % of a monolayer iron on Fe(100) is shown; the solid line is the calculation for the perfect crystal, the broken line is the multiple scattering calculation for configurations of nearest neighbours as shown in Fig. (2). In the lower left panel of Fig. (4) the same comparison is made for 10 % of a monolayer nitrogen added to Fe(100). As can be seen, the influence of the weak scattering nitrogen is much less than that of iron. The average t-matrix approximation gives for adatoms some slightly different results than the site-dependent approximation. This comparison is made in the lower right panel of Fig. (4). The broken line refers here to the average t-matrix approximation.

DISCUSSION

The model calculations show only very small influences of defects in the I-V profiles. The intensities for the vacancy models are generally a bit lower compared to the perfect crystal, as predicted by the kinematic theory. Occasionally there are some small changes in relative peak hights as, for example, in (10) beam from Au(100), where the peak of 100 eV is lowered, while that at 85 eV is evenly enhanced. Such an effect is purely to be attributed to multiple scattering origin.

The intensity from the adatom models is slightly higher than that of the clean crystal, as actually expected, but also here only small changes are visible. All features of the curves are preserved, there is no change in peak positions and the changes in relative peak heights would be undetectable experimentally. Changing the first layer spacing by 2 % has more influence on the I-V curves than 5 or 10 % impurities or vacancies.

The question arises whether this result is representative or not. For vacancies there are no differences between the average t-matrix approximation and the explicit calculation of scattering amplitudes for the neighbouring atoms. This indicates that multiple scattering within a layer is minor at least at normal incidence. For vacancies only nearest neighbours within the plane have been assumed, and for adatoms only nearest neighbours in the next layer. So, only an average for the forward and backward scattering from the defect is accounted

for, thus interferences in the multiple scattering series are damped. A more detailed calculation with spherical clusters around a defect may show some more effects. Also the importance of intralayer scattering should increase at oblique incidence, and point defects might be detectable under these diffraction conditions. Possibly this is one of the reasons, why calculated I-V curves usually don't fit the experimental ones at oblique incidence as well as at normal incidence.

ACKNOWLEDGEMENT

Financial support of the Deutsche Forschungsgemeinschaft (SFB 128) is gratefully acknowledged.

REFERENCES

[1] Henzler, M., Electron diffraction and surface defect structure in electron spectroscopy for surface analysis, ed. by H. Ibach (Springer, Berlin, 1977)

[2] Park, R.L., Houston, J.E., and Schreiner, D.G., The LEED instrument response function, Rev. Sci. Instr. 42 (1971) 60-65
Comsa, G., Coherence length and/or transfer width? Surf. sci. 81 (1979) 57

[3] Wang, G.-C. and Lagally, M.G., Quantitative island size determination in the chemisorbed layer W(110)p(2x1)-O, Surf. Sci. 81 (1979) 69

[4] Moritz, W., Low-energy electron diffraction from disordered surfaces, Inst. Phys. Conf. Ser. No. 41 (1978) 261

[5] Guinier, A., X-ray diffraction (Freeman, San Francisco, 1963)

[6] Beeby, J.L., The diffraction of low-energy electrons by crystals, J. Phys. C1 (1968) 82

[7] Jagodzinski, H., Moritz, W., and Wolf, D., Diffuse LEED intensities of disordered crystal surfaces. I. Correlations between statistics and multiple scattering, Surf. Sci. 77 (1978) 233

[8] Moritz, W., Jagodzinski, H., and Wolf, D., Diffuse LEED intensities of disordered crystal surfaces. II. Multiple scattering on disordered overlayers, Surf. Sci. 77 (1978) 249

[9] See, for example, a recent review article:
Ehrenreich, H. and Schwartz, L.M., The electronic structure of alloys, in Sol. State Physics 31 (1976) (Academic Press, New York, San Francisco, London)

[10] For a detailed description of the theory see: Pendry, J.B., Low-energy electron diffraction (Academic Press, London and New York, 1974)

[11] Tong, S.Y. and Van Hove, M.A., Unified computation scheme of low-energy electron diffraction - the combined space method, Phys. Rev. B16 (1977) 1459

[12] The iron potential was submitted by Moruzzi, V.L. For Au the spin-averaged phase shifts were used as described by Feder, R. and Moritz, W., Relativistic effects on LEED intensities from Au(111), Surf. Sci. 77 (1978) 505

Index